5th International Meeting
on
Wind Turbine Noise
Denver 28 – 30 August 2013

Noise Source Localization On A 8kW Wind Turbine Using A Compact Microphone Array With Advanced Beamforming Algorithms

Rakesh Chandran Ramachandran[*], Hirenkumar Patel, Yong Jiang, Xiaodong Shi, Mahesh Krishnamurthy, and Ganesh Raman[+]. Illinois Institute of Technology, Chicago, USA.

E-mail: rramac4@hawk.iit.edu[*], raman@iit.edu[+]

Summary

It is believed that small wind turbines, which are increasingly being used near residential areas, sound louder than their full scale counterparts due to their close proximity to dwellings. Currently noise measurements on small scale wind turbines are being performed using single microphones which only provide an overall estimate of the total noise emitted from the wind turbine. For wind turbine manufacturers trying to address the issue of noise reduction through design the knowledge of the dominant noise source location and source mechanisms is important. This information can be obtained using microphone arrays and sophisticated beamforming algorithms. In this paper we use a compact microphone array to locate and quantify noise sources on a small Viryd 8000 wind turbine. The results from the microphone array show that we are able to successfully locate both mechanical and aerodynamic noise on the wind turbine using advanced deconvolution algorithms such as TIDY, CLEAN based on Source Coherence (CLEAN-SC), Deconvolution Approach for Mapping Acoustic Sources (DAMAS) and Deconvolution using Linear Programming (LP). For frequencies above 5000 Hz aerodynamic noise appears to be the dominant noise source and for frequencies below 5000 Hz mechanical noise from the nacelle appears to be the dominant noise source. We also performed microphone array measurements on a laboratory test rig of the wind turbine drive train of Viryd 8000. We were able to successfully locate noise sources on various mechanical components in the drive train. The behaviour of the various noise sources are studied at different simulated wind speeds. It was found that gearbox was the dominant noise source.

1. Introduction Wind turbine noise has been one of the primary areas of study when assessing the environmental impact of the wind turbines. Sound is generally one of the most important site constraints for wind turbines. Over the years the regulatory bodies have established certain regulations for the distance between dwellings and wind turbines. Noise measurement on these wind turbines have been typically made using single microphones as per the IEC 61400-11 standard. Most of these types of studies have been performed on full scale utility wind turbines. With the growing need for renewable energy, modern cities are now looking towards developing self sufficient buildings and homes. Small wind turbines are considered to be one of the favourites when it comes to self sustained residential buildings. Since small wind turbines (under 30 kW capacity) are more likely to be closer to human dwellings, the noise from these small wind turbines are typically louder than their larger counterparts. For this reason studies on small wind turbine noise are important. If our goal is to reduce wind turbine noise (especially aerodynamic noise from blades) through design, knowledge of noise source location and its mechanism is necessary. With single microphone measurements this is almost impossible. In order to obtain noise source location estimates, a microphone array with sophisticated beamforming algorithm is required. In this paper we study the noise of a small scale wind turbine (Viryd 8000) using a microphone array (Optinav 24) with

advanced deconvolution algorithms such as TIDY, CLEAN-SC, DAMAS and LP. We will first begin with a brief introduction to wind turbine noise and beamforming. We will then present the details of the wind turbine unit along with the experimental setup used for this study. The results of these experiments will be presented next with detailed discussions and we finally provide a summary of important findings of this study.

1.1 Wind turbine noise The noise radiated from an operating wind turbine could be broadly classified into two categories: 1) Mechanical noise from the nacelle and 2) Aerodynamic noise from the blades. A detailed review of these sound generation mechanisms is provided by Wagner, et al (Wagner, Bareiss, & Guidati, 1996). A summary of these mechanisms is given below.

The mechanical noise originates from the relative motion of mechanical components and from their dynamic response. Various machinery components, such as the generator, gearbox, cooling fans and auxiliary devices contribute to machinery noise. The noise from these sources can propagate directly from the component surface or interior into the air (air-borne). In other cases mechanical noise is transmitted along the structure of the turbine, such as the nacelle casing, tower and rotor blades and radiated from surfaces which may act as loud speakers (structure-borne). Pinder in his work (Pinder, 1992) conducted detailed measurements of mechanical noise of the wind turbines and reported that the main source of machinery noise was the gearbox, and this noise radiates from the nacelle surfaces and machine shaft. Mechanical noise can be both tonal and broadband in nature and is a fixed source.

Aerodynamic noise is radiated from the blades and is mainly associated with the interaction of turbulence with the blade surface. The turbulence may originate either from the natural atmospheric turbulence present in the incoming flow or from the viscous flow in the boundary layer around the blades. There are two mechanisms that gives rise to the aerodynamic noise, namely, (i) inflow turbulence noise and (ii) airfoil self-noise. The inflow turbulence noise is due to the interaction of turbulence in the atmosphere with the leading edge of the blades. Airfoil self-noise arises when an airfoil section encounters a steady, non- turbulent flow field. The two main contributors of this noise are the trailing edge noise and the tip vortex noise. The trailing edge noise is caused by the interaction of the turbulent boundary layer with the trailing edge of the blade. At low Mach numbers, turbulent eddies are inefficient sound sources. If there is a sharp edge close to the eddies they will become more efficient as sound sources. hence the trailing edges of a turbine blade increase the efficiency of the noise radiation from the turbulent eddies in the boundary layer. For a blade of finite length, the pressure difference between the suction and pressure side tends to compensate at the blade tip. This causes a cross flow over the side edge of the tip which creates a tip vortex that is part of the convected wake. The tip vortex noise is known to contribute mostly to high-frequency broadband airfoil self-noise. There has been strong interest in understanding and predicting wind turbine aerodynamic noise in the past. The work on wind turbine noise, particularly aerodynamic noise, has been primarily computational work.

2.2 Beamforming Beamforming is a signal processing technique used for directional signal transmission or reception. The most straight forward way of treating the phased microphone array is classical beamforming. Classical beamforming can be performed in both the frequency domain as frequency domain beamforming (FDBF) and in the time domain as Delay and Sum (DAS). Assuming that the microphone array consists of N microphones, the N x N cross spectral matrix (CSM) 'C' is calculated. Since the locations of the sources are unknown in practice, a scanning grid that covers a region of interest with a certain resolution is formed. The N-dimensional propagation or steering vectors 'g' from each of the grid points to all the N microphones in the array is calculated assuming sources at each of these grid points to be monopole sources of powers 'Y'. Then the source power at grid points are given by equation (1).

$$A = \frac{\sum_{(m,n)} g_m^* C_{mn} g_n}{\sum_{(m,n)} |g_m|^2 |g_n|^2} \tag{1}$$

where the m and n are microphone indices and * represents complex conjugate. The source powers so calculated at every grid point can be plotted to give the beamform map. The conventional beamforming technique performed in the time domain is the DAS technique. In this the time delay for the signal at every grid point to reach each microphone in the array is calculated and is subtracted off the measured signal. These subtracted signals are then summed to give the final beamform map. The beamform maps so formed with the classical beamforming will have poor resolution and side lobes, especially with a compact microphone array.

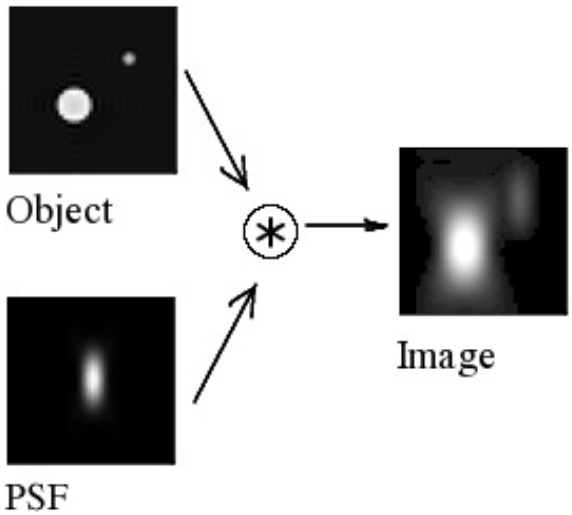

Figure 1. Image illustrating the process on convolution. (Wikipedia, 2006)

In order to obtain a much cleaner beamform map, deconvolution methods are necessary. We can think of the classical beamform map as a convolution or sum of the actual source and its point spread function. The point spread function (PSF) describes the response of an imaging system, in this case the microphone array, to a point source or point object (see Fig. 1). By defining this point spread function of the system and subtracting this out from the classical beamform map we can improve the resolution of the beamform map significantly. This process is known as deconvolution. There are a few widely used deconvolution methods. The deconvolution approach for the mapping of acoustic sources (DAMAS), developed by Brooks and Humphreys (Brooks, 2006) in 2004 is the first such algorithm. The basic concept behind this algorithm is that every point source on the grid will have a point spread function ('A') which is the array's response to the point source that can be obtained synthetically. The beamform map obtained from conventional beamforming ('Y') is assumed to be a result of convolution of the actual source ('X') and its PSF (Y=AX) . Thus by using the PSF and deconvoluting with the conventional beamform map one could obtain a much cleaner beamform map ($X=A^{-1}Y$). This problem could be posed as a non-linear system of equations and solved using iterative techniques such as Gauss-Seidel method. The DAMAS algorithm however is not so efficient on computing time as the PSF have to be calculated for every iteration. This problem was overcome in DAMAS2 (DMS2), suggested by Dougherty (Dougherty, 2005), which uses a shift invariant PSF. The PSF based deconvolution algorithms have the disadvantage that the actual beam patterns of the measured noise signals may not be identical to the ones calculated and will not result in accurate results. This was overcome in the CLEAN algorithm based on spatial coherence (CLEAN-SC), developed by Sijtsma (Sijtsma, 2007), which uses the conventional beamform map as the dirty map and subtracts out the dominant source from the dirty map and iteratively builds a clean map which includes only the most dominant coherent source. A key feature of the CLEAN-SC is its ability to extract absolute power levels from the source plots. Since CLEAN-SC does not use any calculated PSF it is more robust. Another advanced beamforming algorithm named TIDY was developed by Dougherty (Dougherty R. P., 2009). It is philosophically similar to CLEAN-SC, but it works in the time domain using the cross correlation matrix (CCM) instead of the frequency domain which makes use of a CSM, i.e., it

uses the beamform map obtained from the DAS rather than FDBF. Deconvolution using linear programming (LP) uses the simplex method from linear programming to maximize '*c.X*' subject to AX≤Y and X≤0. Here c is a vector of nonnegative weight factors, Y is a vector of sum of the values from the classical beamform map, X is a vector of the unknown source strengths at the selected map points, and A is the point spread function. The new method differs from previous deconvolution algorithms in that the objective function relates directly to the solution, rather than the error in the matching the model function to the beamform map. Detailed discussion of this new algorithm is reported in Dougherty et. al. (Dougherty, Ramachandran, & Raman, 2013).

With this brief introduction to wind turbine noise and beamforming algorithms we will now move on to experimental method used in this work.

(a) (b)

Figure 2. A photograph of (a) Viryd 8000 wind turbine and (b) Optinav 24 microphone array.

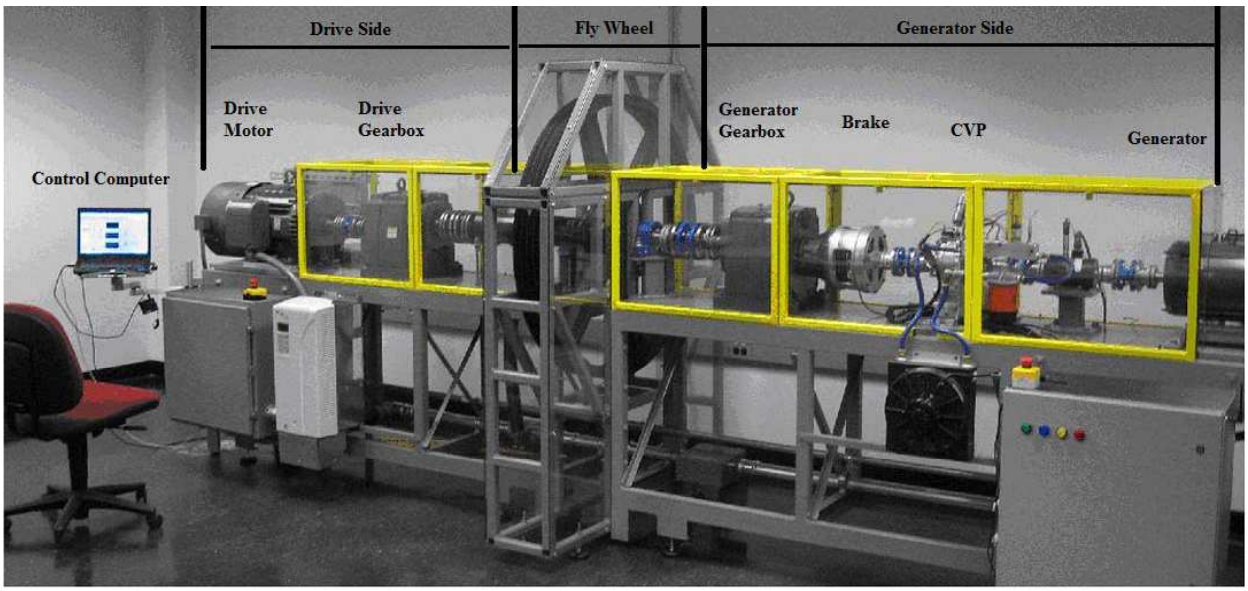

Figure 3. A photograph of the laboratory test rig of Viryd 8000 drive train.

2. Experimental methods

The experimental study was performed on a Viryd 8000 wind turbine with a tower height of 24 m (80 ft) with a rotor diameter of 8.4 m (27.5 ft). The cut-in wind speed of this wind turbine is 4.5 m/s (10 mph) and the cut-out wind speed is 25 m/s (56 mph). The wind turbine has a variable rotor speed of 50 to 150 RPM. The wind turbine has the option to run in a motor mode

as well as generator mode. In the motor mode the unit draws electricity to run the rotor in the nacelle thus producing a constant rpm of the blades. In the generator mode the unit uses the kinetic energy of the wind and converts it to electrical energy using the generator. Measurements were taken with the wind turbine operating in both modes. The wind velocity and direction data were also acquired from the computer log. The yaw mechanism is passive with no furling required. The rated power for this wind turbine is 8 kW at 10m/s. The wind turbine is located in the Stuart field at Illinois Institute of Technology, Chicago, USA. A picture of this wind turbine is shown in Fig. 2(a). The microphone array used for this experiment is an Optinav 24 array with 24 microphones arranged in a log spiral pattern (0.72 m diameter) with a centrally located camera to capture the image of the wind turbine. The signal from the microphone array is acquired by an A/D converter which has 24 I/O audio interfaces. A MAGMA express box handles the task of interfacing the PCI 424 card to the computer. A USB cable connects the camera to a USB port on the computer. A picture of the array is shown in Fig. 2(b). Two locations were chosen for the placement of the microphone array. Location 1 (L1) was at 24 m (80 ft) from the base of the tower and location 2 (L2) was at 15 m (50 ft) from the base of the tower. In order to further explore the mechanical noise sources on the wind turbine, microphone array measurements were made on a laboratory test rig of the Viryd 8000 drive train. It consists of a drive side with a drive motor and gearbox to run a flywheel to replace the blades on an actual wind turbine. A computer program controls the rpm by simulating real life wind speeds and turbulence levels. The generator side is the actual replica of the drive train inside the nacelle of the 8 kW Viryd wind turbine unit. This side consists of a gearbox, brake, continuous variable planetary gearbox (CVP) and the generator. Figure 3 shows the test rig of Viryd 8000 drive train.

3.0 Results and Discussion

Initially the microphone array was qualified in the laboratory by observing the behaviour of the microphone array and various beamforming algorithms when both single and multiple sources are present. Detailed results of these qualification experiments are reported in Ramachandran et. al. (Ramachandran, Raman, & Dougherty, 2011). One of the important findings of the qualification experiment is that the ability of the microphone array and beamforming algorithms in separately locating multiple noise source that are closely spaced depended on the Rayleigh criterion. The Rayleigh criterion is given in equation (2).

$$W = \frac{rD}{\lambda z} \tag{2}$$

where, W =1.22 is the Rayleigh limit which is the distance between the peak and the first zero of an ideal diffraction pattern below which multiple sources cannot be separated when using a particular type of imaging system. In the equation, r is the separation distance between the sources, D is the diameter of the array, λ is the wavelength of the source and z is the distance between the array and the source. The Rayleigh criterion dependence was experimentally demonstrated by Ramachandran et. al. (Ramachandran, Raman, & Dougherty, 2012) As mentioned previously, the diameter of the outermost microphones on the array are 0.72 m. Since the objective of the experiment is to separate mechanical noise from the nacelle and the aerodynamic noise from the blades, we approximate that the aerodynamic noise is close to the tip of the blades and the mechanical noise is at the centre of the nacelle which gives us the source separation distance and the blade length (4.2 m). Now based on the distance between the array and the wind turbine we could estimate the minimum frequency above which the two noise sources could be successfully resolved. For the two locations used in this work, L1 at 24 m and L2 at 15 m the minimum frequency according to Rayleigh limit is estimated to be about 5000 Hz and 4000 Hz, respectively.

We will now look at the data obtained from the wind turbine. Figure 4(a) shows the wind speed and wind direction data obtained simultaneously during the microphone array measurement at location L1. We observe that the average wind speed during this measurement was about 8 m/s with considerable variation in wind direction. Figure 4(b) shows the wind speed and generator power averaged over 10 sec for the same time. We observe that with increase in

wind speed the power generated increases and it decreases with fall in wind speed as expected.

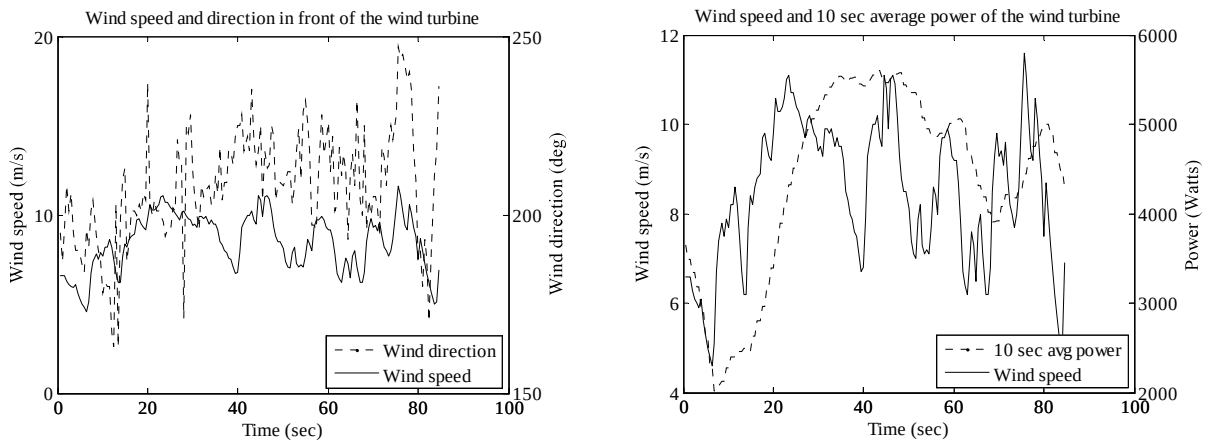

(a) (b)

Figure 4. The wind turbine parameter time record obtained simultaneously during the microphone array measurement at L1 showing (a) wind speed and direction and (b) wind speed and power generated averaged over 10 sec.

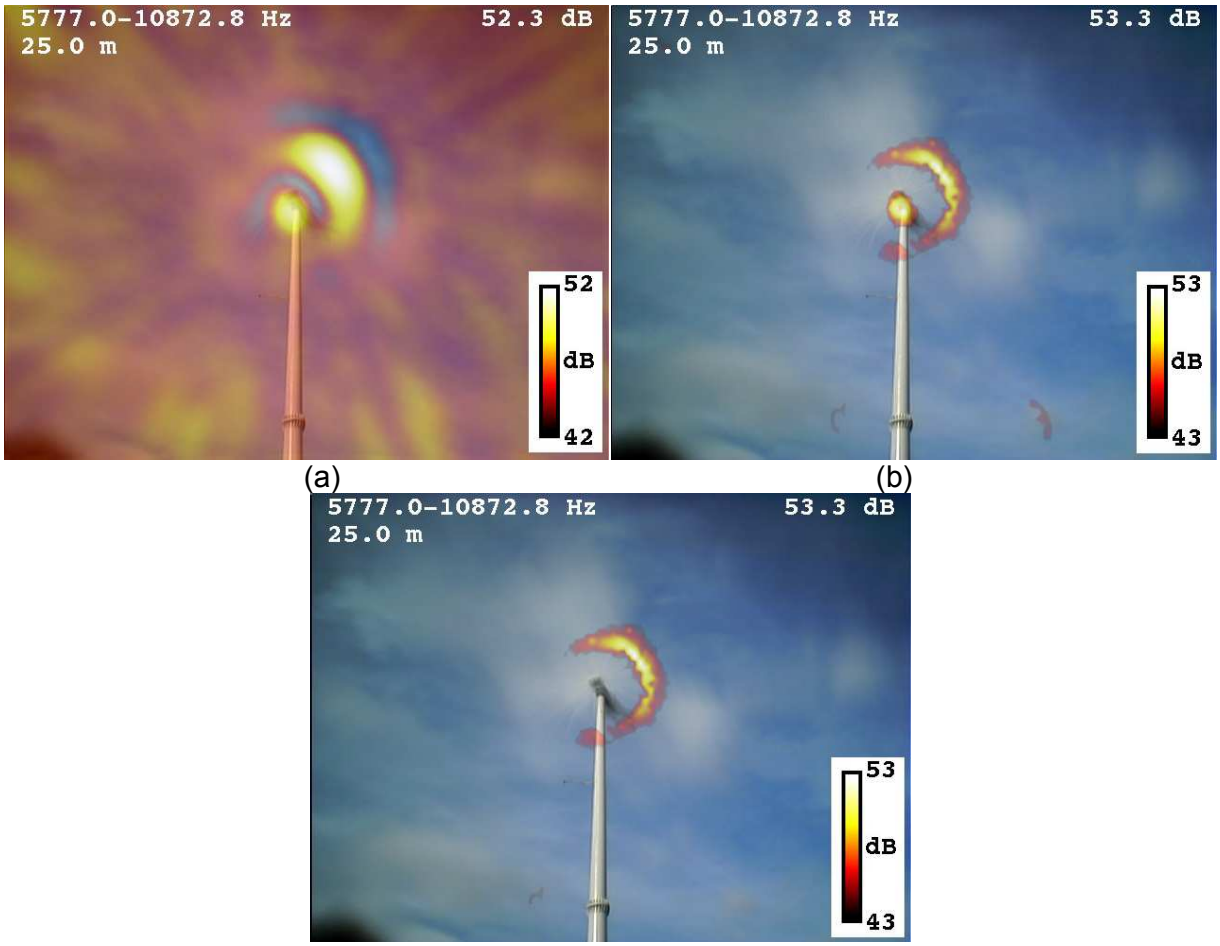

(a) (b)

(c)

Figure 5. Beamform map of wind turbine noise showing the mechanical noise from nacelle and the aerodynamic noise from the blades using (a) DAS and (b) TIDY. The strong asymmetry in the aerodynamic noise about the rotor is shown in (c) using TIDY algorithm.

Figure 5 shows the beamform map (6 – 10 kHz) of the wind turbine noise from location L1 . Since the minimum frequency estimated by Rayleigh limit for L1 is 5000 Hz we begin our analysis above this frequency. Figure 5(a) is the beamform map obtained using the classical

beamforming for the frequency range of 5777 Hz- 10872 Hz averaged over 10 sec. We observe that there are two main noise sources one at the center around the nacelle (mechanical noise) and another towards the tip of the blades (aerodynamic noise). Along with these we also observe a considerable amount of side lobes which is typical of classical beamforming. In order to remove the side lobes and obtain a cleaner beamform map we use advanced deconvolution routines. Figure 5(b) shows the beamform map of the wind turbine noise obtained using TIDY for the same frequency range as Figure 5(a) averaged over 5 sec. We clearly observe the difference between the two beamform maps. The deconvolution routine removed the side lobes completely and produced a cleaner estimate of the noise sources when compared to classical beamforming. On looking at the two beamform maps we observe two interesting features. First, in this frequency range the aerodynamic noise from the blades appear to be more dominant than the mechanical noise from the nacelle. Secondly, the aerodynamic noise appears to be asymmetric about the axis of the rotor. The reason behind the asymmetry of the aerodynamic noise is the convective or Doppler amplification effect. Similar behaviour was observed by Oerlemans et. al. (Oerlemans, Sijtsma, & Mendez Lopez, 2007) and Ramachandran et. al. (Ramachandran, Raman, & Dougherty, 2012) on full scale wind turbines separately. Figure 5(c) shows the aerodynamic noise from the blades showing the strong asymmetry about the rotor axis using TIDY algorithm averaged over 5 sec. We observe that the noise from the blades appear to be at a higher amplitude during the blade's downward motion and at a lower amplitude as the blade moves upwards. This is due to the Doppler amplification where the noise appears to be louder when the noise is convected towards the observer on the ground than when the noise is convected away from the observer.

Next we look at the wind turbine parameters for another case where the microphone array was located at L2. Figure 6(a) shows the wind speed and direction record obtained simultaneously during the microphone array measurement at location L2. We observe that the wind speed changes considerably towards the end. It jumps from an average of about 9 m/s to 12 m/s. Figure 6(b) shows the wind speed and generated power averaged over 10 sec during the same time. Similar observations are made as before where the power increases with an increase in velocity and vice versa.

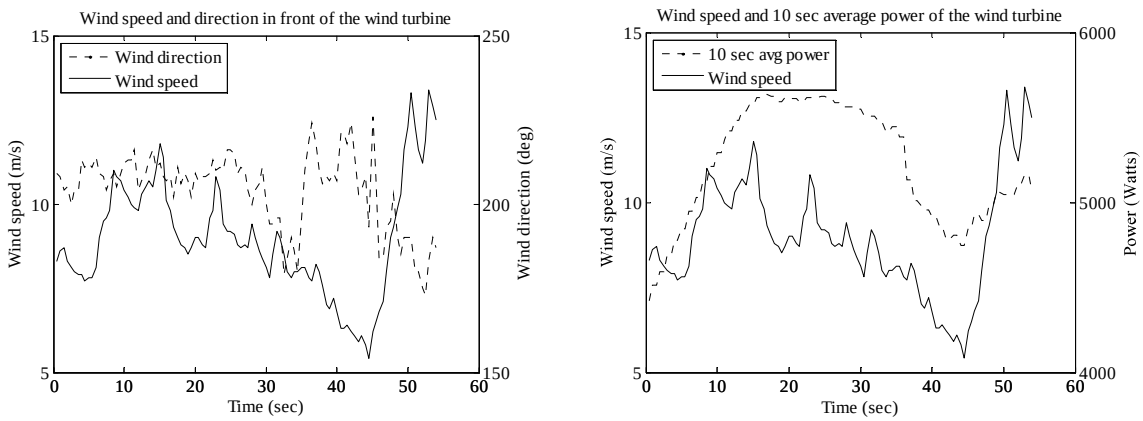

(a) (b)

Figure 6. The wind turbine parameter time record obtained simultaneously during the microphone array measurement at L2 showing (a) wind speed and direction and (b) wind speed and power generated averaged over 10 sec.

Figure 7 shows the beamform map of the wind turbine noise at a particular instant during its revolution to look at the noise sources individually and instaneously. The frequency of interest here is 6120 Hz- 7314 Hz which is well above the minimum frequency estimated by Rayleigh criterion for L2 (4000 Hz). The beamform map was obtained using the TIDY algorithm. Here we observe that there are two weak sources and one dominant source. The dominant noise source appears to be emitting from the blade that is on its downward motion. As explained before this is due to the Doppler amplification effect. One of the two weak sources appears to be emitting from the blade that has completed its upward motion and is beginning its motion downward (at

the top). The second weak source appears to be emitting from the nacelle and is most likely the noise due to the dynamic interaction of the various mechanical components inside the nacelle. This further supports our understanding that in this frequency range (above 5000 Hz) the aerodynamic noise is the dominant noise source and is most likely the trailing edge noise of the blades.

Figure 7. Beamform map of the wind turbine noise at location L2 using TIDY algorithm at a particular instant during its revolution.

In order to understand the noise sources at lower frequencies (lower than Rayleigh limit) we require deconvolution routines which could successfully work under the Rayleigh limit. DAMAS and Linear Programming (LP) algorithms have shown the ability to work under the Rayleigh limit. Figure 8 compare the beamform maps of wind turbine noise at a frequency around 3000 Hz using classical beamforming 8(a) and various deconvolution routines (TIDY 8(b), CLEAN-SC 8(c), DAMAS 8(d) and LP 8(e)). From Figure 8 we observe that the classical beamforming fails to provide conclusive location estimates for noise sources on the wind turbine. The TIDY algorithm provides a poor estimate where we could see two broad peaks, one around the nacelle and another close to the tip of the blades. The CLEAN-SC algorithm clearly separates these two sources and we observe that the dominant noise source is the mechanical noise from the nacelle with only weak aerodynamic noise being present. The beamform maps obtained from DAMAS and LP have better resolution than CLEAN-SC and we observe a similar result as CLEAN-SC. The results from DAMAS and LP are similar but the computation time for LP is 1/10th that of DAMAS.

We explore further by looking at a lower frequency (around 2 kHz). Figure 9 shows the beamform maps of wind turbine noise around 2 kHz using classical beamforming 9(a) and various deconvolution routines (TIDY 9(b), CLEAN-SC 9(c), DAMAS 9(d) and LP 9(e)). Once again we observe that the beamform map from classical beamforming is inconclusive and TIDY algorithm shows an extended source which is again inconclusive. CLEAN-SC locates the mechanical noise from the nacelle but does not provide any location estimates for aerodynamic noise. DAMAS and LP show the nacelle noise to be the dominant again at this frequency and they also show weak sources around the nacelle which are most likely the aerodynamic noise sources from the blades. However noise estimates from DAMAS and LP at lower frequencies (less than 1000 Hz) begin to degrade and becomes inconclusive.

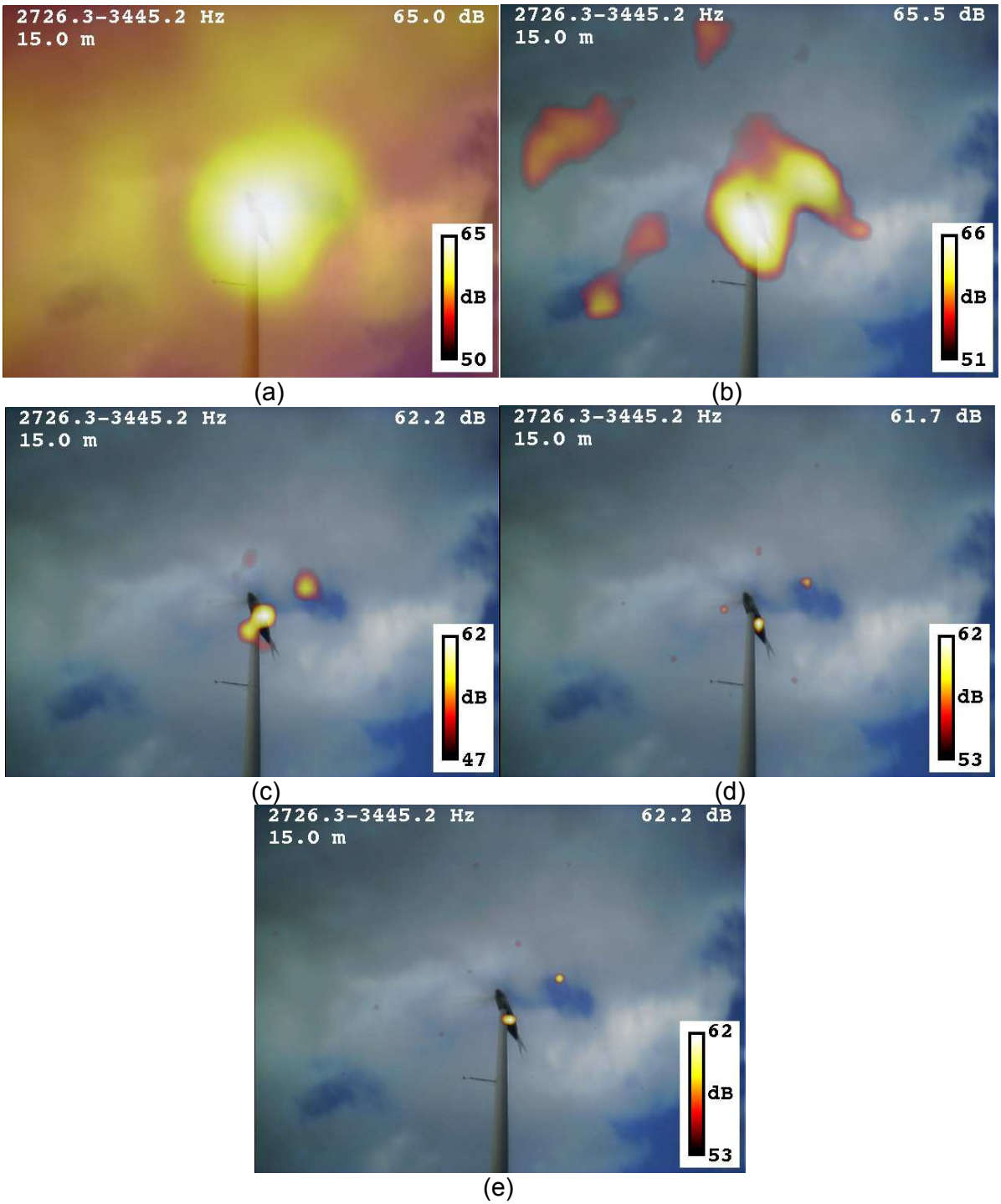

Figure 8. Beamform map of wind turbine noise around 3 kHZ using (a) Classical Beamforming, (b) TIDY, (c) CLEAN-SC, (d) DAMAS and (e)LP.

In order to further understand the behavior of various mechanical noise sources inside the nacelle we conducted microphone array measurements on the laboratory test rig of the Viryd 8000 wind turbine. The microphone array was located 0.75 m from the drive train. The noise measurements were made at 1 m/s interval starting from 6 m/s to 16 m/s. Figure 10 shows the beamform map of the noise from gearbox, brake, CVP and generator using the TIDY algorithm with the drive train operating at a simulated wind speed of 6 m/s. We observe that using the microphone array and beamforming the individual noise sources were located on the drive train and quantified. Figure 11 shows the peak noise levels from the gearbox, brake, CVP and generator with the wind turbine drive train operating at various simulated wind speeds. We observe from this figure that for the most part the dominant noise source is the gearbox. We also observe that for wind speeds less than 10 m/s the generator was the dominant noise

source. We also observe that for the gearbox and brake there is an increase in peak noise level with increase in wind speed, whereas for the generator and CVP we observe a slight decrease in peak noise level. Another interesting observation is that above the simulated wind speed of 10 m/s the noise levels of the various components remain stable. We believe that this is due to the fact that the wind turbine drive train is designed to generate a constant power for a wind speed of 10 m/s. This can be observed from the power curve of the Viryd 8000 as shown in Figure. 12. We observe that the power starts increasing from about 6 m/s and becomes constant at 8 kW at around 10 m/s.

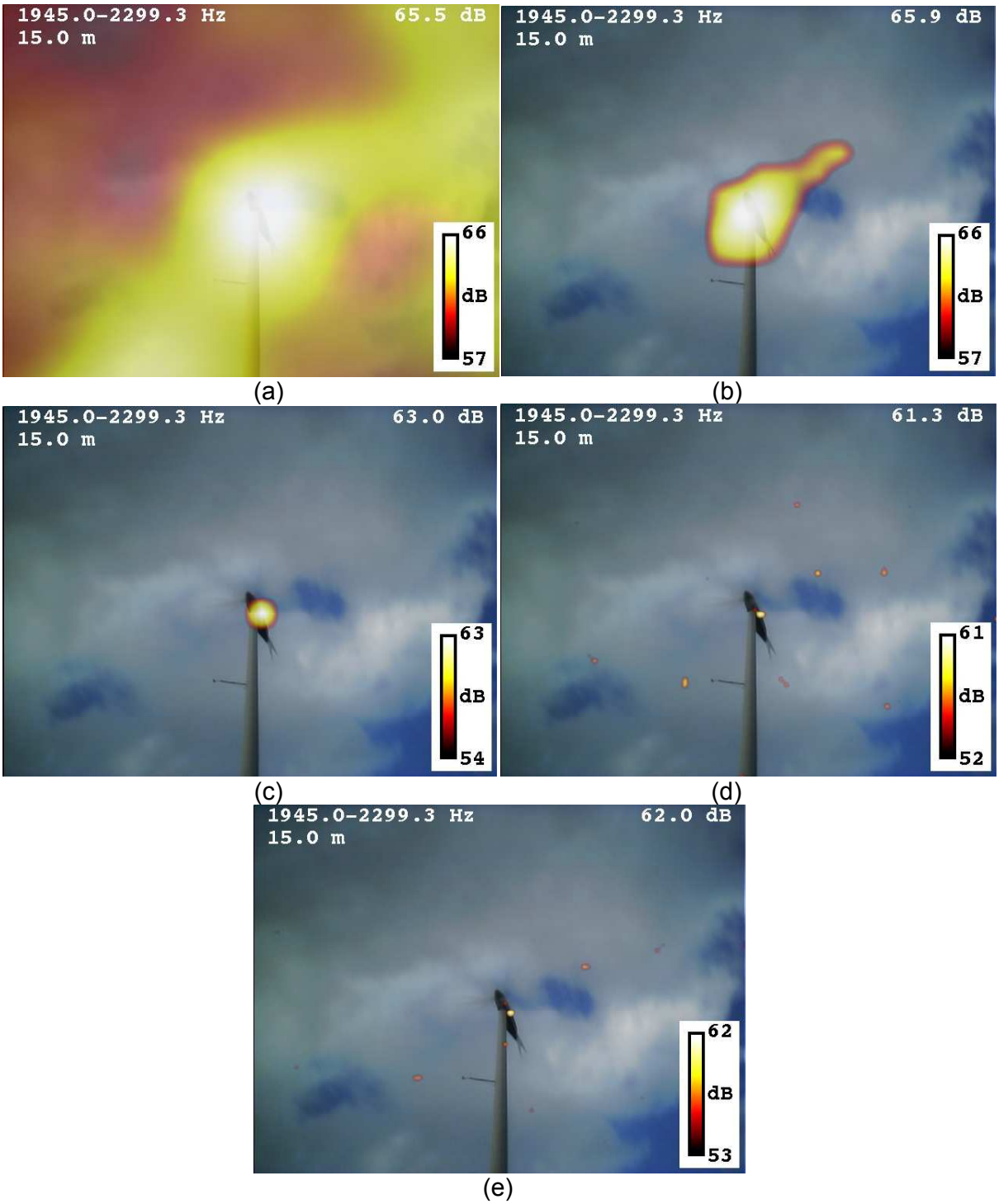

Figure 9. Beamform maps of wind turbine noise around 2 kHz using (a) classical beamforming, (b) TIDY, (c) CLEAN-SC, (d) DAMAS and (e) LP.

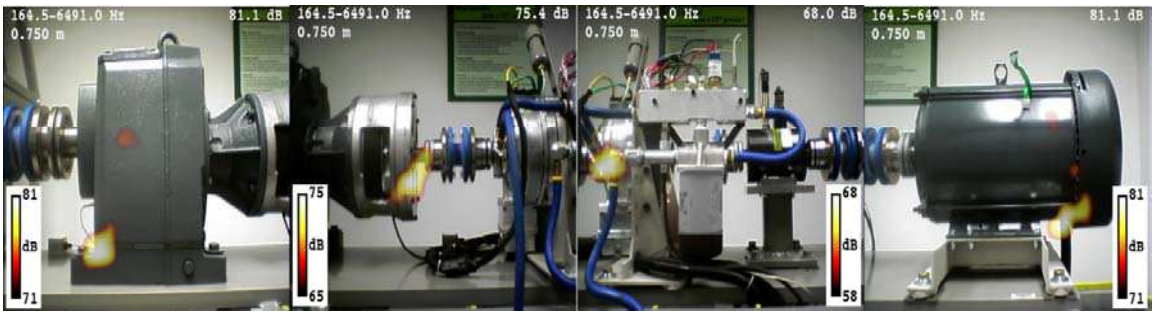

Figure 10. Beamform maps of (a) gearbox, (b) brake, (c) CVP and (d) generator with the drive train operating at a simulated wind speed of 6 m/s using TIDY algorithm.

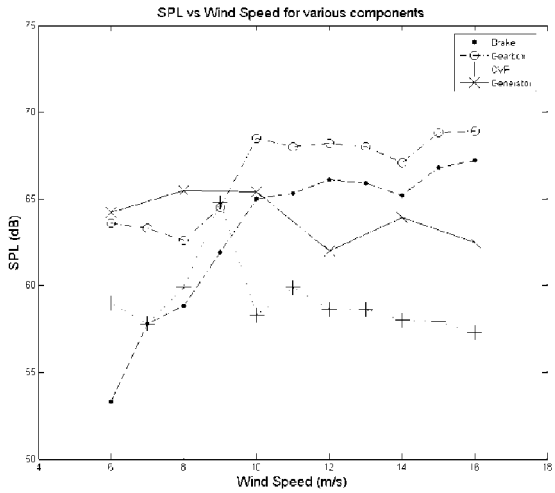

Figure 11. Plot showing the behavior noise from various mechanical components of the wind turbine drive train with change in wind speed.

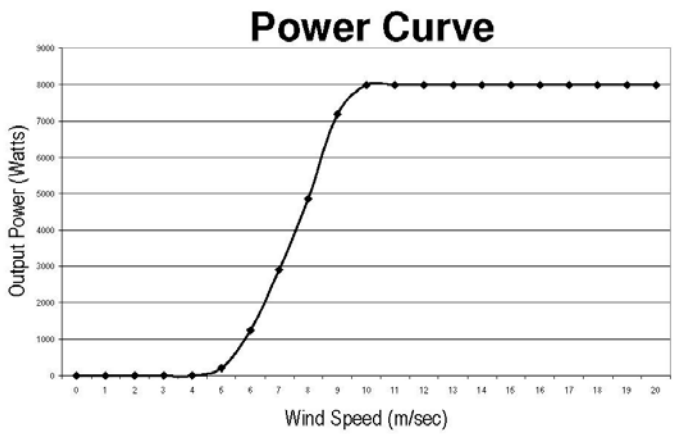

Figure 12. Power curve of Viryd 8000 wind turbine.

4.0 Conclusions

This study uses a unique method to locate the noise sources on a small scale wind turbine. A compact microphone array was used for the study along with sophisticated beamforming algorithms. It was found that the ability of the microphone array to resolve multiple noise sources depended on the Rayleigh criterion. For frequencies above this Rayleigh limit we observed that classical beamforming analysis provided results with considerable side lobes and we required an advanced deconvolution technique (TIDY) to obtain clean results. At frequencies above 5000 Hz we observed that the aerodynamic noise from blades were the dominant noise source when compared to the mechanical noise from the nacelle. For frequencies lower than the Rayleigh limit we found that classical beamforming produced

inconclusive location estimates and we had to use super resolution algorithms such as DAMAS and LP to resolve the noise sources. Here we observed that the dominant noise source is the mechanical noise from the nacelle with weak aerodynamic noise. In order to further understand the behaviour of various mechanical components inside the nacelle, experiments were conducted on a laboratory test rig of the Viryd 8000 wind turbine drive train. The measurements were made with different simulated wind speeds. It was found that the gearbox was the dominant noise source of the drive train. We also observed that the noise from the various components varied between 6 m/s to 10 m/s after which they were stable. This was attributed to the fact that the drive train was designed for a stable operation above 10 m/s as evident from the power curve of the wind turbine. In sum, the microphone array with beamforming is a unique and powerful method to locate and quantify noise sources on a small scale wind turbine and is useful in understanding the physics behind the noise generation on wind turbines.

Acknowledgements

This work was supported in part by the U.S. Department of Energy under Grant DE-EE 0002979.

References

Brooks, T. F., & Humphreys, J. W. (2006). A Deconvolution Approach for the Mapping of Acoustic Sources. *Journal of Sound and Vibration* , 856-879.

Dougherty, R. P. (2005). Extension of DAMAS and Benefits and Limitations of Deconvolution in Beamforming. *AIAA-2005-2961.* Monterey, California: 11th AIAA/CEAS Aeroacoustics Conference.

Dougherty, R. P. (2009). Improved Phased Array Imaging of Model Jet. *AIAA 2009-3182.* Miami, FL.

Dougherty, R. P., Ramachandran, R. C., & Raman, G. (2013). Deconvolution of Sources in Aeroacoustic Images from Phased Microphone Arrays Using Linear Programming. *19th AIAA/CEAS Aeroacoustics Conference.* Berlin.

Oerlemans, S., Sijtsma, P., & Mendez Lopez, B. (2007). Location and Quantification of Noise Sources on a Wind Turbine. *Journal of Sound and Vibration* , 869-883.

Pinder, J. N. (1992). Mechanical Noise from Wind Turbines. *Wind Engineering* , 158-168.

Ramachandran, R. C., Raman, G., & Dougherty, R. P. (2011). Evaluation of Various Beamforming Algorithms for Wind Turbine Noise Measurement. *49th AIAA Aerospace Sciences Meeting,.* Orlando, FL: AIAA 2011-2388.

Ramachandran, R. C., Raman, G., & Dougherty, R. P. (2012). Noise source localization using a compact microphone array: Studies on a Full Scale Wind turbine in a wind farm. *Wind Engineering* , 589-604.

Sijtsma, P. (2007). CLEAN based on spatical source coherence. *International Journal of Aeroacoustics* , 357-374.

Wagner, S., Bareiss, R., & Guidati, G. (1996). *Wind Turbine Noise.* Berlin: Springer.

Wikipedia. (2006). *Convolution illustrated: longitudinal (XZ) central slice of a 3D image acquired by a fluorescence microspoce*. Retrieved from http://en.wikipedia.org/wiki/File:Convolution_Illustrated_eng.png